Structure−Property Correlation on Second Hyperpolarizabilities of Symmetric One-Center and Three-Center Radicals

Satoru Yamada, Masayoshi Nakano,* and Kizashi Yamaguchi

Department of Chemistry, Graduate School of Science, Osaka University, Toyonaka, Osaka 560-0043, Japan

Received: April 21, 1999; In Final Form: June 30, 1999

In order to elucidate the features of the second hyperpolarizabilities (γ) for *n*-center radical systems (*n*, integer), we investigate the γ of symmetric one-center radical models, i.e., BH_3^-, CH_3, and NH_3^+, and three-center radical models, i.e., $BH(CH_2)_2^-$, $CH(CH_2)_2$, and $NH(CH_2)_2^+$, by various electron-correlation and a density functional methods using extended basis sets. Since these models are isoelectronic systems involving 9 and 23 electrons, respectively, the γ values are expected to reflect the features of their charge density distributions. It is actually found that the γ values for the isoelectronic systems sensitively depend on their charged states. For instance, the one-center radicals exhibit positive γ values at high-order electron correlation level using sufficiently large basis sets, while, for the three-center radicals, only $NH(CH_2)_2^+$ is found to possess negative γ. These features are analyzed using γ density plots, which can provide a local view of spatial contributions of electrons to the γ, and are discussed in relation to our structure-property correlation rule.

1. Introduction

The third-order nonlinear optical properties for many organic compounds have been actively studied both experimentally and theoretically[1−4] because of their large nonlinearity and fast responses. In particular, the second hyperpolarizability (γ), which is the origin of a macroscopic third-order nonlinear optical response, has been investigated using quantum mechanical calculations.[2] In previous papers,[5,6] we have presented a structure−property correlation rule of γ and proposed a criterion of exhibiting a negative γ. This criterion states that the systems with large contribution of symmetric resonance structure with inversible polarization (SRIP) to the ground state tend to exhibit negative γ. The sign of γ is known to be important in quantum optics: the positive value causes the self-focusing effect of an incident beam, while the negative one does the self-defocusing effects.[7] It is also well-known that most organic nonlinear optical systems exhibit positive γ. Therefore, the design and the investigation of the molecular systems with negative γ are considered to provide profounder insight into the mechanism of the third-order nonlinear optical processes for organic molecular systems. On the basis of our structure−property correlation rule, we proposed a new class of third-order nonlinear optical compounds, nitronyl nitroxide radical (NNR), the longitudinal γ of which is predicted to be negative using ab initio molecular orbital (MO) calculations involving high-order electron correlation effects.[8] We also investigated the γ values for phenyl nitronyl nitroxide radical (PNNR) systems involving the NNR using semiempirical MO methods, and elucidated that the large negative γ values originate in the electron fluctuation in the NNR unit.[9] A series of such molecular systems is known to be thermally stable and to include molecules exhibiting attractive magnetic properties.[10] Recently,[11] an analog involving the NNR, i.e., 2-phenyl-4,4,5,5-tetramethylimidazoline-3-oxide-1-oxyl (PTIO), was experimentally investigated and its off-resonant γ value was found to be negative (in order 10^{-35}−10^{-34} esu) in conformity with our prediction.

In general, most of organic third-order nonlinear optical molecules have been closed-shell systems and so far only a few open-shell (radical) systems have been investigated. As mentioned above, however, radical systems are expected to have negative γ as well as other attractive properties. In this study, we consider two types of symmetric radical molecular models from the viewpoint of our structure−property correlation rule on γ. We investigate γ for isoelectronic one-center radicals, i.e., BH_3^-, CH_3, and NH_3^+, and three-center radicals, i.e., $BH(CH_2)_2^-$, $CH(CH_2)_2$, and $NH(CH_2)_2^+$, using ab initio MO and a density functional (DF), i.e., B3LYP,[12] methods. These models have a possibility of exhibiting the SRIP though the degree of its contribution to the ground state of each system is different from each other. Since the systems with large SRIP contribution tend to exhibit remarkable electron-correlation dependence of γ,[6,8] various electron-correlation methods are applied to the calculations of the γ and the results are analyzed using γ density plots,[13] which can elucidate a local spatial contribution of electrons to the γ. From our previous studies,[4,8] the magnitude, signs, and electron-correlation dependences of γ for radical systems are found to sensitively reflect the difference in the charge distributions and the degree of SRIP contribution. Therefore, we confine our attention to the elucidation of the relations among the charged states, the degree of SRIP contributions, and the spatial contribution to the γ of these radical systems.

The present paper is organized as follows. In section 2, we briefly explain our structure−property correlation rule for γ. In section 3, we explain the calculation and analysis methods and show possible SRIP for the molecular model systems. The results of one- and three-center radicals are discussed in connection with our structure−property correlation rule in sections 4 and 5, respectively. This is followed by a conclusion in section 6.

* Corresponding author.

10.1021/jp9913158 CCC: $18.00
Published on Web 08/17/1999

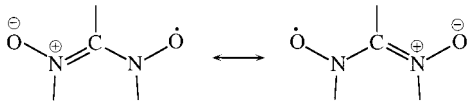

Figure 1. Symmetric resonance structures with inversible polarization (SRIP) for nitronyl nitroxide radical (NNR).

2. Virtual Excitation Process and Structure−Property Correlation Rule for Third-Order Nonlinear Optical Systems

The γ can be described by the fourth-order virtual excitation processes in the perturbation theory.[7] The perturbative formula for γ can be approximately partitioned into three types of contributions (the first term (I), the second term (II), and the third term (III) in the right-hand side of eq 1) as[14]

$$\gamma = \sum_{n=1} \frac{(\mu_{n0})^2(\mu_{nn})^2}{E_{n0}^3} - \sum_{n=1} \frac{(\mu_{n0})^4}{E_{n0}^3} + \sum_{\substack{m,n=1 \\ (m\neq n)}} \frac{(\mu_{n0})^2(\mu_{mn})^2}{E_{n0}^2 E_{\mathrm{m0}}} \quad (1)$$

where μ_{n0} is the transition moment between the ground and the nth excited states, μ_{mn} is the transition moment between the mth and the nth excited states, μ_{nn} is the difference of dipole moments between the ground and the nth excited states, and E_{n0} is the transition energy given by $(E_n - E_0)$. From these equations, apparently, the contributions of types (I) ($\gamma^{(\mathrm{I})}$) and (III) ($\gamma^{(\mathrm{III})}$) are positive in sign, whereas the contribution of type (II) ($\gamma^{(\mathrm{II})}$) is negative. For conventional molecular compounds with large positive γ, there are two characteristic cases: (i) $|\gamma^{(\mathrm{I})}| \gg |\gamma^{(\mathrm{II})}| \approx |\gamma^{(\mathrm{III})}|$ ($\gamma > 0$) and (ii) $|\gamma^{(\mathrm{I})}| = 0$, $|\gamma^{(\mathrm{II})}| < |\gamma^{(\mathrm{III})}|$ ($\gamma > 0$). In case (i), the compounds have large nonsymmetric charge distributions which are responsible for large μ_{nn}, whereas in case (ii), the compounds are centrosymmetric systems in which the contributions of type (I) disappear. In the third case, i.e., (iii) $|\gamma^{(\mathrm{I})}| = 0$, $|\gamma^{(\mathrm{II})}| > |\gamma^{(\mathrm{III})}|$ ($\gamma < 0$), the systems exhibit negative static γ. Such systems are symmetric ($\mu_{nn} = 0$) and exhibit strong virtual excitation between the ground and the nth excited states ($|\mu_{0n}| > |\mu_{nm}|$). In case (iii), the systems have the large contribution of resonances between polarized structures with mutually opposite directions. That is, the large contributions of the stable resonance structures with large dipole moments correspond to a reduction of the E_{n0} between the ground and the allowed first excited states with large contributions from the resonance structures and to an enhancement of the magnitude of the μ_{n0} between the ground and the allowed first excited states. As a result, a system with a large contribution of symmetric resonance structures with inversible polarization, i.e., SRIP, satisfies our criteria for the system to have a negative γ. We have already proposed some π-conjugated systems with large SRIP contribution, e.g., charged soliton-like oligomer,[13] NNR,[8,9,15] anion radical state of pentalene,[6] and cation radical state of tetrathiafulvalene (TTF).[16] As an example, the SRIP of the NNR is shown in Figure 1. These γ values are predicted to be negative in sign by ab initio MO calculations including high-order electron-correlation effects.

3. Calculated Molecules, Calculation Methods, and Analysis Method

3.1. Calculated Molecules and Calculation Methods. The one-center radical models, i.e., BH_3^-, CH_3, and NH_3^+, have 9 electrons. Therefore, the features of γ are expected to reflect the feature of each charged state. The one-center radical models are assumed to be planar structures. Their geometries are optimized using the B3LYP method with 6-311G(3d2f,3p2d) basis set.[17] Ab initio MO and the B3LYP calculations in this study are performed by the GAUSSIAN 94 program package.[16] Figure 2 shows possible SRIP of the one-center radicals. Although each optimized structure takes an equilateral triangle (r(B−H) = 1.2118 Å, r(C−H) = 1.0776 Å, and r(C−H) = 1.0237 Å), we only consider the structure changes by SRIP in the direction x since we focus on the γ_{xxxx} component in this study. It is well-known that the use of extended basis sets, which are augmented by diffuse and polarization functions, is indispensable for reproducing semiquantitative γ, especially for small systems. To elucidate basis set dependence of γ for these systems, we employ some standard and extended basis sets involving diffuse p, d, and/or f functions on B, C, and N atoms and diffuse s and/or p functions on H atom. All the exponents of these diffuse functions are determined by the even-tempered method (see Table 1). The inner polarization functions are represented in parentheses and the diffuse functions are represented by the notation, e.g., +p/d. It is noted that the functions before "/" are set on B, C, and N atoms, while the functions after "/" are on H atom. For the inner polarization functions in parentheses, the function before "," are set on B, C, and N atoms, while the functions after "," are on H atom.

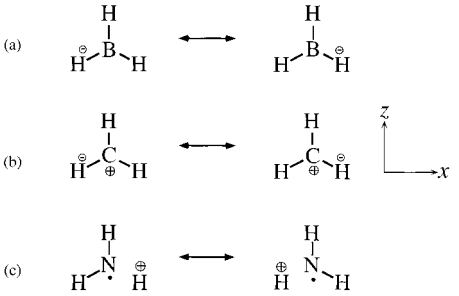

Figure 2. Symmetric resonance structures with inversible polarization (SRIP) for one-center radicals: (a) BH_3^- (r(B−H) = 1.2118 Å), (b) CH_3 (r(C−H) = 1.0776 Å), and (c) NH_3^+ (r(C−H) = 1.0237 Å). These molecular geometries are optimized using B3LYP method with 6-311G(3d2f,3p2d).

The three-center radical models, i.e., $BH(CH_2)_2^-$, $CH(CH_2)_2$, and $NH(CH_2)_2^+$, are assumed to be planar structures in order to clarify the contribution of π-electrons to the γ. Figure 3 shows the possible SRIP for the three-center radicals. The geometries of the three-center radicals are optimized using the B3LYP method with 6-311G(2d,2p) basis set.[17] For the calculation of γ, we use the standard 6-311G and 6-311G(d,p) basis sets and extended basis sets augmented by diffuse f function on B, C, and N atoms and diffuse d function on H atom (see Table 1).

It was also found that the electron-correlation effects on γ are significantly large for open-shell systems.[6,8,18] In order to elucidate the electron-correlation dependences of γ for these systems, we perform the Møller−Plesset perturbation methods (MP2, MP3, MP4DQ, MP4SDQ, and MP4SDTQ) and the coupled-cluster methods (CCD, CCSD, and CCSD(T)). The Hartree−Fock (HF), the MP2, the quadratic configuration interaction (QCISD), and the B3LYP methods are applied to the construction of γ density plots. It is noted that the QCISD method is known to be able to reproduce the total energy calculated by the CCSD method satisfactorily. Here the symbols S, D, T, and Q denote the inclusion of the correlation effects caused by the single, double, triple, and quadruple excitations, respectively. The CC and QCI methods can include these correlation effects to the infinite order.

TABLE 1: Exponential Gaussian Orbital Parameters for Diffuse Functions Added on the 6-311G Basis Set

	B			C			N			H		
	p	d	f	p	d	f	p	d	f	s	p	d
+p/s	0.0310			0.0483			0.0590			0.0324		
+d/p		0.0310			0.0483			0.0590			0.0324	
+pd/sp	0.0310	0.0310		0.0483	0.0483		0.0590	0.0590		0.0324	0.0324	
+f/d			0.0310			0.0483			0.0590			0.0324
+pf/sd	0.0310		0.0310	0.0483		0.0483	0.0590		0.0590	0.0324		0.0324

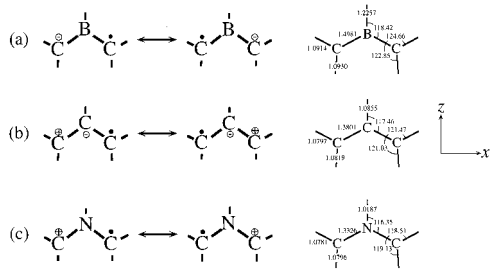

Figure 3. Symmetric resonance structures with inversible polarization (SRIP) for three-center radicals: (a) $BH(CH_2)_2^-$, (b) $CH(CH_2)_2$, and (c) $NH(CH_2)_2^+$. These molecular geometries are optimized using B3LYP method with 6-311G(2d,2p).

The total Hamiltonian in the presence of a uniform electric field $\boldsymbol{F}$ is expressed as

$$H = H_0 + \sum_i \boldsymbol{F}\cdot\boldsymbol{r}_i - \sum_I Z_I \boldsymbol{F}\cdot\boldsymbol{R}_I \tag{2}$$

where indices i and I signify electrons and nuclei, respectively. Z_I is the atomic number of the Ith nucleus and H_0 is the field-free Hamiltonian. The total energy can be obtained as the expectation values for the wave functions Ψ in the presence of the field.

$$E = \langle\Psi|H|\Psi\rangle \tag{3}$$

Similarly, the dipole moment is expressed as

$$\mu = \langle\Psi|\sum_I Z_I \boldsymbol{R}_I - \sum_i \boldsymbol{r}_i|\Psi\rangle \tag{4}$$

Differentiation of eq 2 with respect to F^i gives

$$\frac{\partial E}{\partial F^i} = \left\langle \frac{\partial \Psi}{\partial F^i}\middle| H \middle|\Psi\right\rangle + \left\langle \Psi\middle| \frac{\partial H}{\partial F^i}\middle|\Psi\right\rangle + \left\langle \Psi\middle| H \middle| \frac{\partial \Psi}{\partial F^i}\right\rangle \tag{5}$$

If Ψ is the true wave function, the first and third terms on the right-hand side of eq 5 is equal to zero by the Hellmann−Feynman theorem.[19] The variational methods such as CHF satisfy the theorem. If the Hellmann−Feynman theorem is satisfied, the dipole moment defined by eq 4 can be expressed as

$$\mu^i = -\partial E/\partial F^i \tag{6}$$

In general, the total energy and dipole moment can be expanded as the power series of the applied field:

$$E = E_0 - \sum_i \mu_0^i F^i - {}^1/_2 \sum_{ij} \alpha_{ij} F^i F^j - {}^1/_3 \sum_{ijk} \beta_{ijk} F^i F^j F^k - {}^1/_4 \sum_{ijkl} \gamma_{ijkl} F^i F^j F^k F^l - \ldots \tag{7}$$

$$\mu^i = \mu_0^i + \sum_j \alpha_{ij} F^j + \sum_{jk} \beta_{ijk} F^j F^k + \sum_{jkl} \gamma_{ijkl} F^j F^k F^l - \ldots \tag{8}$$

where μ_0^i is the permanent dipole moment. The Hellmann−Feynman theorem asserts that eqs 7 and 8 are compatible. For the nonvariational methods such as MP and CC, the Hellmann−Feynman theorem is not satisfied. Practically, however, there are little computational differences between the hyperpolarizabilities in these two expansions.[20] In this study, we use the definition of hyperpolarizability based on eq 7.

We confine our attention to the *xxxx* components of γ, γ_{xxxx}, for the model systems since relations among γ_{xxxx} and the resonance structures with polarization in the direction are primarily considered in this study. The γ_{xxxx} are calculated by the numerical differentiation of the total energy E with respect to the applied field by

$$\gamma_{xxxx} = \{E(3F^x) - 12E(2F^x) + 39E(F^x) - 56E(0) + 39E(-F^x) - 12E(-2F^x) + E(-3F^x)\}/\{36(F^x)^4\} \tag{9}$$

Here, $E(F^x)$ indicates the total energy in the presence of the field F applied in the x direction. This method is referred to as the finite-field (FF) method. In order to avoid numerical errors, we use several minimum field strengths. After numerical differentiations using these fields, we adopt a numerically stable γ_{xxxx}, which is found to be obtained by using fields 0.001−0.003 au for these systems.

3.2. Hyperpolarizability Density Analysis. In this section, we provide a brief explanation of γ density and the method for analysis using its spatial plot. This analysis is useful for obtaining pictorial and intuitive understanding of the spatial contribution to γ.[8,13,18]

The charge density function $\rho(\boldsymbol{r},\boldsymbol{F})$ can be expanded in powers of the field F as

$$\rho(\boldsymbol{r},\boldsymbol{F}) = \rho^{(0)}(\boldsymbol{r}) + \sum_j \rho_j^{(1)}(\boldsymbol{r}) F^j + \frac{1}{2!}\sum_{jk} \rho_{jk}^{(2)}(\boldsymbol{r}) F^j F^k + \frac{1}{3!}\sum_{jkl} \rho_{jkl}^{(3)}(\boldsymbol{r}) F^j F^k F^l + \ldots \tag{10}$$

From this equation and the expansion formula of the dipole moment in powers of the field (eq 8), the static γ can be expressed by

$$\gamma_{ijkl} = -\frac{1}{3!}\int \boldsymbol{r}^i \rho_{jkl}^{(3)}(\boldsymbol{r})\, \mathrm{d}\boldsymbol{r}^3 \tag{11}$$

where

$$\rho_{jkl}^{(3)}(\boldsymbol{r}) = \left.\frac{\partial^3 \rho}{\partial F^j \partial F^k \partial F^l}\right|_{F=0} \tag{12}$$

This third-order derivative of the electron density with respect to the applied electric fields is referred to as the γ density. In this study, we confine our attention to the γ_{xxxx} densities ($\rho_{xxx}^{(3)}(\boldsymbol{r})$) corresponding to γ_{xxxx}, which are calculated at each

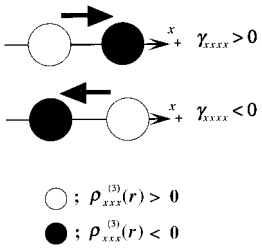

Figure 4. Schematic diagram of the second hyperpolarizability (γ_{xxxx}) densities $\rho^{(3)}_{xxx}(\boldsymbol{r})$. The size of circle represents the magnitude of $\rho^{(3)}_{xxx}(\boldsymbol{r})$ and the arrow shows the sign of γ_{xxxx} determined by the relative spatial configuration between these two $\rho^{(3)}_{xxx}(\boldsymbol{r})$.

spatial point in the discretized space by using the following third-order numerical differentiation formula.

$$\rho^{(3)}_{xxx}(\boldsymbol{r}) = \{\rho(\boldsymbol{r},2F^x) - \rho(\boldsymbol{r},-2F^x) - 2(\rho(\boldsymbol{r},F^x) - \rho(\boldsymbol{r},-F^x))\}/2(F^x)^3 \quad (13)$$

where $\rho^{(3)}_{xxx}(\boldsymbol{r})$ represents the charge density at a spatial point $\boldsymbol{r}$ in the presence of the field F^x.

In order to explain the analysis procedure by using the γ_{xxxx} densities ($\rho^{(3)}_{xxx}(\boldsymbol{r})$), let us consider a pair of localized $\rho^{(3)}_{xxx}(\boldsymbol{r})$ shown in Figure 4. The positive sign of the $\rho^{(3)}_{xxx}(\boldsymbol{r})$ implies that the second derivative of the charge density increases with the increase in the field. The arrow from a positive to a negative $\rho^{(3)}_{xxx}(\boldsymbol{r})$ shows the sign of the contribution determined by the relative spatial configuration between the two $\rho^{(3)}_{xxx}(\boldsymbol{r})$. That is, the sign of the contribution becomes positive when the direction of the arrow coincides with the positive direction of the coordinate system. The contribution determined by the $\rho^{(3)}_{xxx}(\boldsymbol{r})$ of the two points is more significant, when their distance is larger.

4. γ and γ Densities of One-Center Radical Models

It is predicted from Figure 2 that the SRIP contributions to the stability of the ground states of CH_3 and NH_3^+ are small since the resonance structures have unstable features of the charge separation (for CH_3 shown in Figure 2b) and the bond breaking (for NH_3^+ shown in Figure 2c). Although the SRIP contribution of BH_3^- (Figure 2a) is somewhat expected, the Coulomb repulsion due to the extra electron in the resonance structures may reduce the SRIP contribution.

4.1. Basis Set Dependency. Figure 5 shows electron-correlation and basis-set dependences of γ_{xxxx} for the one-center radicals. Figure 5, a, c, and e, shows the augmentation effects of diffuse functions to the 6-311G basis set on γ_{xxxx}, and Figure 5, b, d, and f, shows the augmentation effects of inner polarization functions to the 6-311G+*f*/*d* basis set on γ_{xxxx}. It is found that one-center radicals, especially BH_3^-, have large basis set dependences. As shown in Figure 5a, the difference in the types of adding diffuse and polarization functions is considered to change a degree of enhancement of the electron-correlation effects on γ of BH_3^-. That is, the augmentations of diffuse p/s and d/p functions are shown to slightly enhance the electron-correlation effects on γ_{xxxx} of BH_3^-, while the augmentation of diffuse f/d functions are shown to enormously enhance the effects. The augmentation of inner polarization d/p functions is also shown to enhance the electron-correlation effects on γ_{xxxx} of BH_3^- (see Figure 5b). However, only a slight difference is shown between the electron-correlation dependence of γ_{xxxx} of BH_3^- by 6-311G(2d,2p)+f/d basis set and that by 6-311G(3d,3p)+f/d basis set. This indicates that the effect of adding diffuse and polarization functions on γ_{xxxx} for BH_3^- is sufficiently converged at the 6-311G(3d,3p)+f/d basis set level.

For CH_3 (see Figure 5, c and d), the tendency of electron-correlation dependences of γ_{xxxx} using various basis sets is shown to be similar to each other though the magnitude of γ_{xxxx} is different from each other. The augmentations of diffuse functions are shown to enhance the magnitude of γ_{xxxx} of CH_3 (see Figure 5c). Although the augmentation of a set of inner polarization d/p functions to 6-311G is shown to significantly enhance the magnitude of γ_{xxxx} for CH_3, the further augmentations of the inner polarization d/p functions to 6-311G(d,p)+f/d are shown to reduce the magnitude of the γ_{xxxx} (see Figure 5d). As a result, the use of both diffuse f/d functions and inner polarization d/p functions are found to be indispensable for reproducing reliable γ_{xxxx} for this system.

As shown in Figure 5e, the magnitude of γ_{xxxx} for NH_3^+ by using extended basis sets is shown to be larger than that by using standard 6-311G basis set at all electron-correlation levels. However, the feature of variation in γ_{xxxx} of NH_3^+ for different electron-correlation methods depends on the types of extended basis sets used. For instance, the γ_{xxxx} of NH_3^+ obtained using 6-311G+d/p basis set at the MP*n* ($n = 2-4$) and the CC levels are smaller than those at the HF level, while the γ_{xxxx} using 6-311G+f/d basis set at the CC levels are larger than those at the HF level. The electron-correlation dependences of γ_{xxxx} for NH_3^+ by using 6-311G+f/d, 6-311G+pf/sd, and 6-311G+df/pd are similar to each other. On the contrary, as shown in Figure 5f, the electron-correlation dependences of γ_{xxxx} for NH_3^+ using the extended basis sets augmented by inner polarization d/f functions to the 6-311G+f/d basis set are shown to be quite different from each other. This feature can be presumed by the fact that the augmentations by inner polarization functions are important for the description of the electronic states of cation radical, i.e., NH_3^+. However, electron-correlation dependence of γ_{xxxx} for NH_3^+ is shown to become small at the 6-311G(3d,3p)+f/d basis set level. This suggests that the large-size basis set somewhat compensates the deficiency in electron-correlation correction at the low-order levels obtained by smaller basis sets.

Judging from these basis-set dependences of the γ_{xxxx}, the 6-311G(3d,3p)+f/d basis set is expected to provide qualitatively converged electron-correlation dependences of γ_{xxxx} for each one-center radical model. Therefore, the 6-311G(3d,3p)+f/d is used in the next section.

4.2. Electron-Correlation Dependency. As shown in Figure 5, there are remarkable differences in the magnitude and electron-correlation dependences of γ_{xxxx} for these radicals calculated by 6-311G(3d,3p)+f/d basis set. The $|\gamma_{xxxx}|$ of BH_3^- is found to be the largest, while that of NH_3^+ is found to be the smallest. A remarkable electron-correlation dependence is observed for BH_3^-. All the MP*n* ($n = 2-4$) methods provide large negative γ_{xxxx} for BH_3^- (Figure 5b), while the CC methods provide positive γ_{xxxx}. This indicates that higher-order electron correlation methods, i.e., CCSD method at least, are found to be indispensable for obtaining qualitatively converged γ_{xxxx} of BH_3^-. That is, the S and D effects up to infinite order are predicted to have significant influence on the qualitative γ_{xxxx} for BH_3^-. From the comparison of CCSD and CCSD(T) results, the T effects are found to slightly change the γ_{xxxx} at the CCSD level. For CH_3 (see Figure 5d), although the electron-correlation effects on the γ_{xxxx} are not small, the electron-correlation effects beyond the MP2 level are considered to be relatively small. The electron-correlation dependence of γ_{xxxx} for NH_3^+ (see Figure 5f) is obviously small compared with that for other radicals. It is found from these results that the features of the

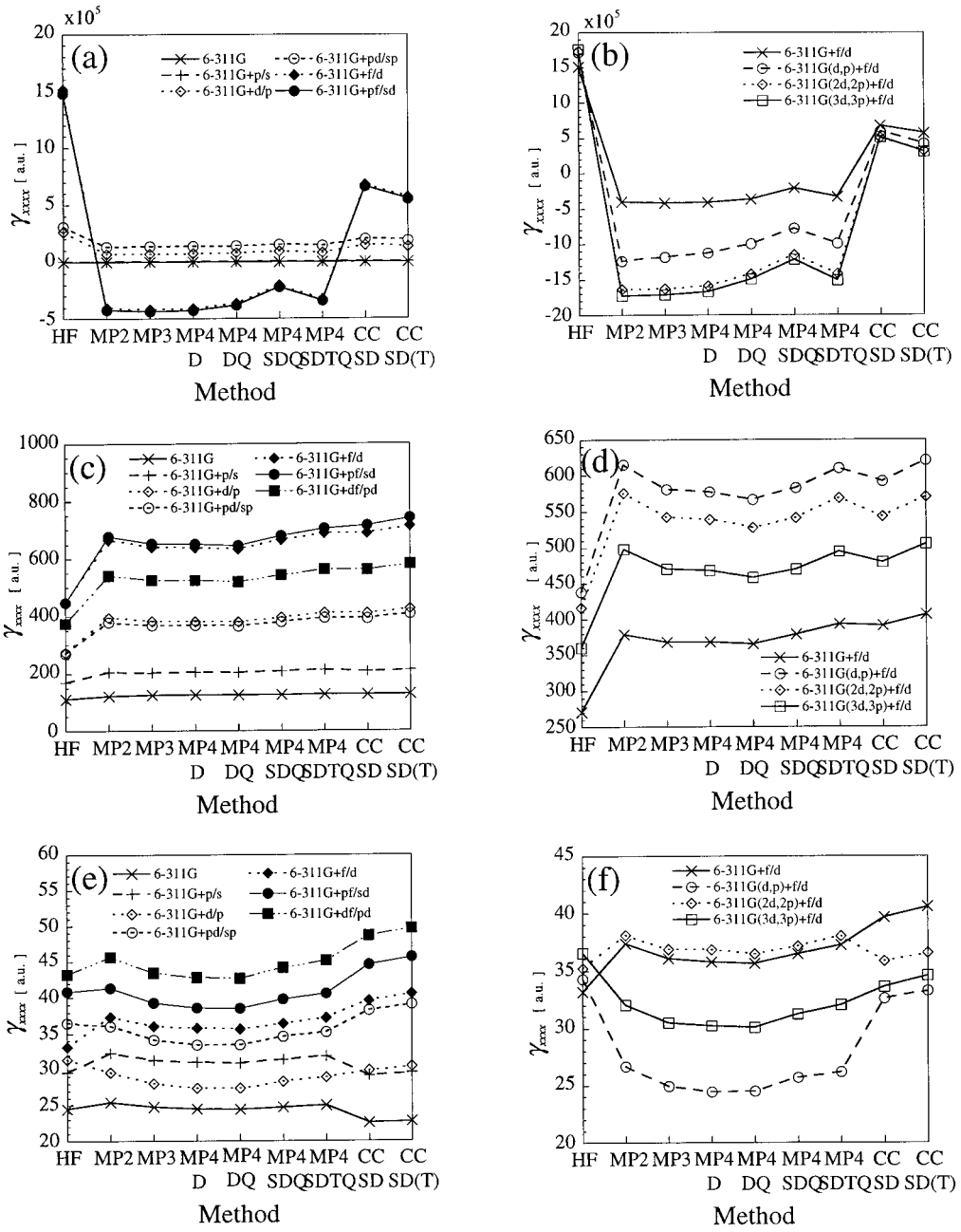

Figure 5. Variations in the γ_{xxxx} of three-center radicals ((a) and (b) for BH_3^-, (c) and (d) for CH_3, and (e) and (f) for NH_3^+) for various basis sets and electron-correlation methods. The γ_{xxxx} values at the QCISD/6-311G(3d,3p)+f/d are 791 000 au (BH_3^-), 480 au (CH_3), and 40.4 au (NH_3^+). The γ_{xxxx} values at the B3LYP/6-311G(3d,3p)+f/d are 1 000 000 au (BH_3^-), 550 au (CH_3), and 46.5 au (NH_3^+).

electron-correlation dependences of γ_{xxxx} are strongly depend on the charged states for these radicals.

The remarkable electron-correlation dependence of γ_{xxxx} for BH_3^- is considered to originate in the SRIP contribution (see Figure 2a) to the ground state of BH_3^-. However, the sign of γ_{xxxx} for BH_3^- at the CCSD(T) level is shown to be positive. If the SRIP of BH_3^- contributed significantly to the stability of the ground state, BH_3^- would have negative γ_{xxxx}. As predicted previously, therefore, the SRIP contribution for BH_3^- is considered not to be so large. This implies that the resonant structures are not so stable. This feature is considered to be caused by the strong Coulomb repulsion due to the extra electron in the resonant structures of BH_3^-.

4.3. γ Density Analysis. Figures 6−8 show the results of γ_{xxxx} density analysis and γ_{xxxx} values for the one-center radicals by using HF, MP2, QCISD, and B3LYP methods. All the γ density distributions are obtained using extended 6-311G(3d, 3p)+f/d basis set. A plane at which the γ_{xxxx} densities are drawn is located at 1.0 au above the molecular plane since we focus on the contribution of π-electrons to the γ_{xxxx}.

Figure 6 shows that all the γ_{xxxx} density distribution patterns of BH_3^- are similar to each other, except for the case at the MP2 level. The inner regions of γ_{xxxx} densities obtained by the HF, QCISD, and B3LYP methods exhibit negative contribution, while the outer regions exhibit positive contributions, which mainly determine the total γ_{xxxx}. The sign of γ_{xxxx} density distribution of BH_3^- obtained by the MP2 method is shown to be opposite to that by other methods. The γ_{xxxx} density distribution at the MP2 level reflects the lower-order electron-correlation effects (MPn ($n = 2-4$)) on the γ_{xxxx} of BH_3^- (see Figure 5b), the effects of which make the γ_{xxxx} of BH_3^- negative in sign. The outer γ_{xxxx} density distribution regions at the QCISD level are shown to reduce (Figure 6c) compared with those at the HF level (Figure 6a). This indicates that the electron-

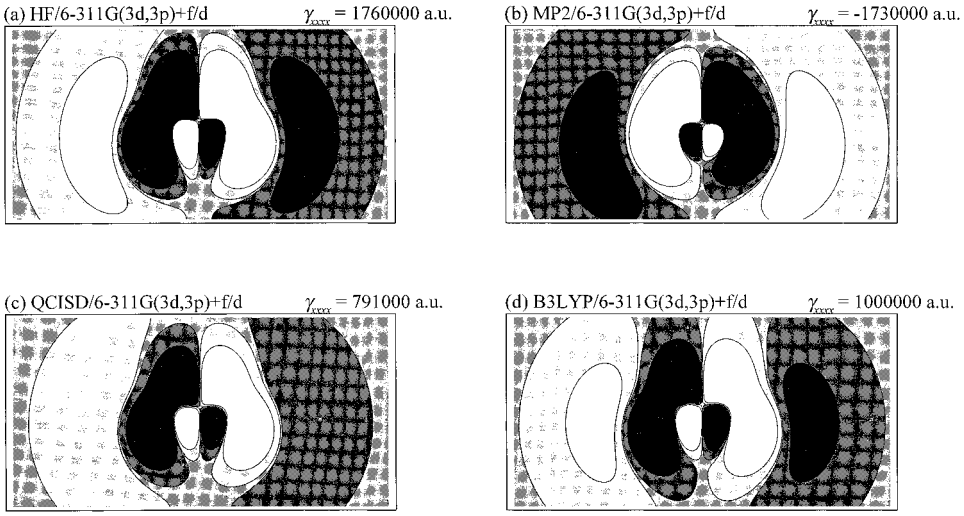

Figure 6. Contour plots of $\rho^{(3)}_{xxx}(\boldsymbol{r})$ distribution on the plane located at 1.0 au above the molecular plane for BH_3^-. Contours are drawn at 100.0, 10.0, −10.0, and −100.0 au. Lighter areas represent the spatial regions with larger $\rho^{(3)}_{xxx}(\boldsymbol{r})$ values.

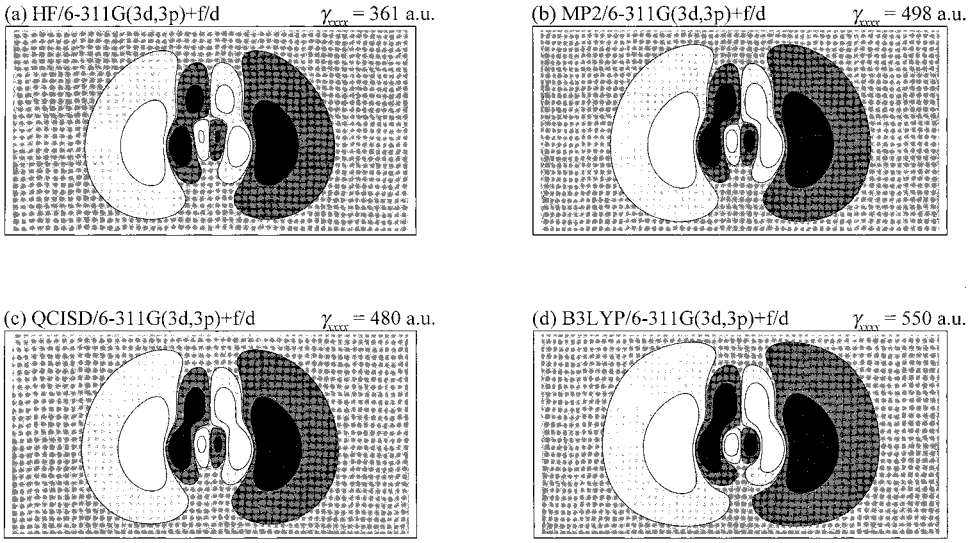

Figure 7. Contour plots of $\rho^{(3)}_{xxx}(\boldsymbol{r})$ distribution on the plane located at 1.0 au above the molecular plane for CH_3. Contours are drawn at 1.0, 0.1, −0.1, and −1.0 au. Lighter areas represent the spatial regions with larger $\rho^{(3)}_{xxx}(\boldsymbol{r})$ values.

correlation effect at the QCISD level significantly decreases the positive contribution to γ_{xxxx} of BH_3^-, the effect of which causes the fact that the magnitude of γ_{xxxx} for BH_3^- at the QCISD level decreases compared with that at the HF level. As shown in Figure 6d, the γ_{xxxx} density distribution and the γ_{xxxx} value of BH_3^- at the B3LYP level are shown to more similar to those at the QCISD level than those at the HF level. This suggests that the B3LYP method can well reproduce the qualitative electron-correlation effects on γ_{xxxx} for BH_3^- at the QCISD level at least.

Figure 7 shows the γ_{xxxx} density distribution of CH_3. In a comparison of the γ_{xxxx} density distribution of CH_3 at the HF level (Figure 7a) with that at the MP2 level (Figure 7b), the electron-correlation effect at the MP2 level on the γ_{xxxx} density distribution is shown to slightly enhance the outer γ_{xxxx} density region, which provides dominant positive contribution to the total γ_{xxxx}. This causes the increase in the magnitude of γ_{xxxx} (Figure 5d). As seen from the γ_{xxxx} density distributions of CH_3 at the MP2 (Figure 7b) and the QCISD levels (Figure 7c), there is no great difference in the electron-correlation effects on γ_{xxxx} densities of CH_3 at the MP2 and QCISD levels. This feature supports the electron-correlation dependence of γ_{xxxx} for CH_3 (Figure 5d). The γ_{xxxx} density distribution of CH_3 obtained using the B3LYP method (Figure 7d) is also shown to be similar to those using the QCISD method though the γ_{xxxx} density distribution regions at the B3LYP level are somewhat enhanced compared with those at the QCISD level. As a result, the electron-correlation effects on γ_{xxxx} of CH_3 at the B3LYP level is considered to be qualitatively similar to those of CH_3 at the MP2 and the QCISD levels.

Figure 8 shows the γ_{xxxx} density distributions of NH_3^+. All the distributions are shown to be much similar to each other. There are found to be two dominant outer density distribution regions, which provide a positive contribution to the γ_{xxxx}. The electron-correlation effects are shown to just provide slight changes in the magnitude of γ_{xxxx} density distributions of NH_3^+. These slight changes in the γ_{xxxx} density distributions well reflect the moderate electron-correlation dependence of γ_{xxxx} for NH_3^+ (see Figure 5f).

As can be seen from the γ_{xxxx} density distributions of these one-center radicals at the QCISD level (Figures 6c, 7c, and 8c), the qualitative distribution patterns are similar to each other, and an essential difference in the γ_{xxxx} density distributions is observed in their magnitudes. That is, the dominant γ_{xxxx} density distribution of BH_3^-, particularly in the outer region, which has

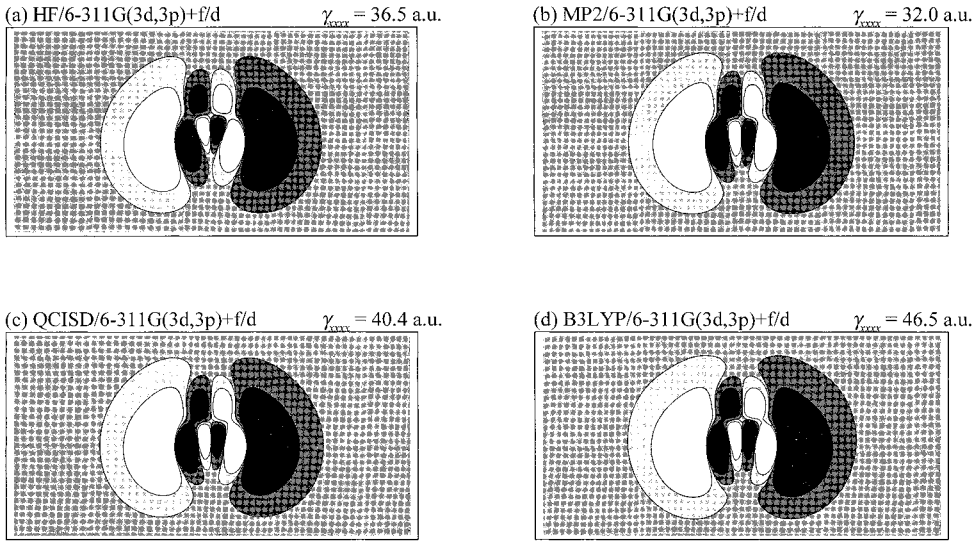

Figure 8. Contour plots of $\rho^{(3)}_{xxx}(\boldsymbol{r})$ distribution on the plane located at 1.0 au above the molecular plane for NH_3^+. Contours are drawn at 0.10, 0.010, −0.010, and −0.10 au. Lighter areas represent the spatial regions with larger $\rho^{(3)}_{xxx}(\boldsymbol{r})$ values.

the largest $|\gamma_{xxxx}|$ in these three radicals, is considered to be much larger than that of NH_3^+, which has the smallest $|\gamma_{xxxx}|$ in these three radicals. Apparently, this feature reflects the fact that the anion radical has an extended charge distribution compared with the cation radical.

It is found that the one-center anion radical (BH_3^-) has a positive γ_{xxxx}, originating in the outer γ_{xxxx} density distributions at the high-order electron-correlation level, though that has somewhat SRIP contribution (Figure 2a), which relates to the negative contributions of inner γ_{xxxx} distributions (Figure 6). This suggests that the SRIP contribution in BH_3^- is reduced due to strong Coulomb repulsion in the resonance structures and that an excess electron in BH_3^- significantly enhances the positive contribution originating in the virtual excitation processes involving high-lying excited states (type (III) in eq 1).

It is concluded that the magnitude, signs, and electron-correlation dependences of γ_{xxxx} for one-center radicals sensitively reflect the difference in the charge distributions and the degree of SRIP contribution.

5. γ and γ Densities of Three-Center Radical Models

As shown in Figure 3, $CH(CH_2)_2$ is not expected to have large SRIP contribution by the destabilization of the resonance structures due to the charge separation, while $BH(CH_2)_2^-$ and $NH(CH_2)_2^+$ are expected to have large SRIP contributions. Judging from the case of one-center anion radical (BH_3^-), however, it is predicted that the SRIP contribution of $BH(CH_2)_2^-$ is reduced, while an excess electron in $BH(CH_2)_2^-$ significantly enhances the positive contribution (given by type (III) in eq 1). Thus, the γ_{xxxx} of $BH(CH_2)_2^-$ is predicted to be positive in sign. As a result, only $NH(CH_2)_2^+$ is expected to have a negative γ_{xxxx}.

5.1. Basis Set Dependency. Figure 9 shows basis sets and electron-correlation dependences of γ_{xxxx} for the three-center radicals. Since the basis set dependences are known to be reduced for the γ in the longitudinal direction of larger-size systems,[21] the effects of the augmentation of diffuse functions to the 6-311G basis set on the γ_{xxxx} are mainly investigated. From the results of the one-center radicals, the extended basis set used here, 6-311G+f/d, is considered to be sufficient for elucidating the qualitative electron-correlation dependences of γ_{xxxx}. Figure 9a shows that the augmentation of diffuse functions remarkably enhances the electron-correlation effects on γ_{xxxx} of $BH(CH_2)_2^-$, especially at the higher-order electron-correlation levels, i.e., CCSD and CCSD(T) levels. That is, the signs of γ_{xxxx} for $BH(CH_2)_2^-$ obtained using extended basis sets, 6-311G+f and 6-311G+f/d, are found to be negative as well as those using standard basis sets, 6-311G and 6-311G(d,p), at all the MPn ($n = 2-4$) levels, while at the CC levels the γ_{xxxx} values using the extended and standard basis sets are found to be positive and negative, respectively.

As shown in Figure 9b, the γ_{xxxx} values for $CH(CH_2)_2$ obtained using the extended basis sets, 6-311G+f and 6-311G+f/d, are much larger than those using the standard basis sets, 6-311G and 6-311G(d,p), at all the electron-correlation levels though both the calculation methods using extended and standard basis sets provide positive γ_{xxxx}. In contrast, for the γ_{xxxx} of $NH(CH_2)_2^+$, the calculation methods using the standard and extended basis sets provide similar values at all the electron-correlation levels (see Figure 9c).

The difference in the basis set dependences of γ_{xxxx} for $BH(CH_2)_2^-$ and $NH(CH_2)_2^+$ is considered to reflect that in the charge distribution for each charged state of these radicals. Since a charge distribution region of the anion radical ($BH(CH_2)_2^-$) is considered to be larger than that of the cation radical ($NH(CH_2)_2^+$), the augmentation of diffuse functions is considered to be more important for obtaining the qualitatively converged electron-correlation dependence of γ_{xxxx} for $BH(CH_2)_2^-$ than for $NH(CH_2)_2^+$.

Since the extended basis sets, 6-311G+f and 6-311G+f/d, are found to provide similar γ_{xxxx} and the electron-correlation dependences of γ_{xxxx} for these systems, the results calculated using 6-311G+f/d basis set are employed in the following discussion on electron-correlation dependences of γ_{xxxx} and their density distributions for these systems.

5.2. Electron-Correlation Dependency. As shown in Figure 9a, a remarkable electron-correlation dependence is observed for $BH(CH_2)_2^-$. All the MPn ($n = 2-4$) methods provide negative γ_{xxxx} for $BH(CH_2)_2^-$, while the CC methods provide large positive γ_{xxxx}. Although such remarkable electron-correlation dependences of γ_{xxxx} for $BH(CH_2)_2^-$ suggest the existence of SRIP contribution, the higher-order electron-correlation methods are found to provide large positive γ_{xxxx} for $BH(CH_2)_2^-$. This indicates that the positive contribution of γ_{xxxx} (type (III)

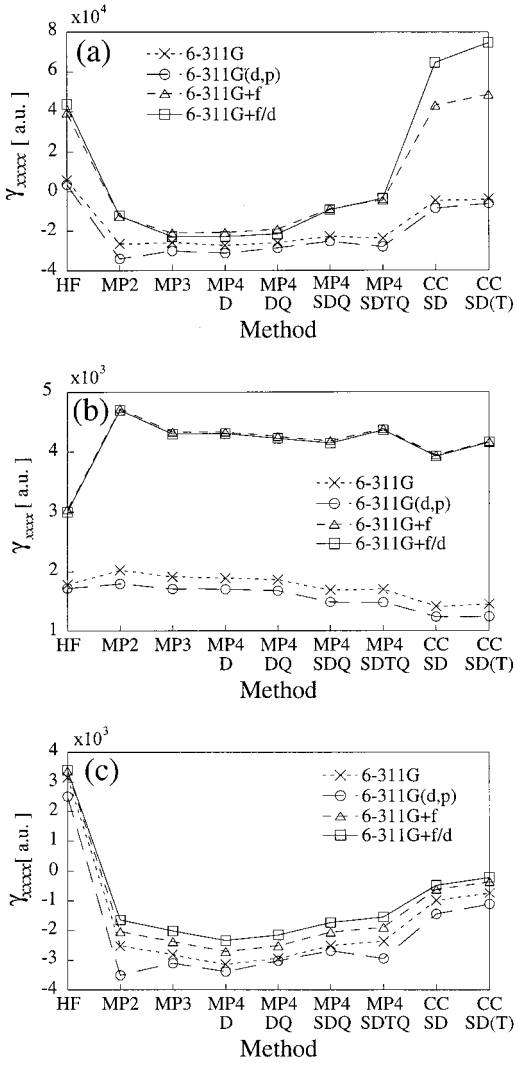

Figure 9. Variations in the γ_{xxxx} of three-center radicals ((a) $BH(CH_2)_2^-$, (b) $CH(CH_2)_2$, and (c) $NH(CH_2)_2^+$) for various basis sets and electron-correlation methods. The γ_{xxxx} values at the QCISD/6-311G+f/d are 85 600 au ($BH(CH_2)_2^-$), 3950 au ($CH(CH_2)_2$), and −361 au ($NH(CH_2)_2^+$). The γ_{xxxx} values at the B3LYP/6-311G+f/d are 93200 au (BH_3^-), 3890 au ($CH(CH_2)_2$), and −419 au ($NH(CH_2)_2^+$).

in eq 1) for $BH(CH_2)_2^-$ exceeds the negative contribution of the γ_{xxxx} (type (II) in eq 1) at the higher-order electron-correlation levels, i.e., CC levels. The decrease in type (II) contribution is considered to be caused by the reduction of SRIP contribution owing to strong Coulomb repulsion in the resonance structures as in the case of BH_3^-. The large type (III) contribution of γ_{xxxx} for $BH(CH_2)_2^-$ is presumed to reflect the extended charge distribution, which enhances the contribution of the virtual excitation process (type (III)) involving higher-lying excited states. This presumption is considered to be also supported by the remarkable basis set dependence of γ_{xxxx} particularly at the CC levels for $BH(CH_2)_2^-$ (see Figure 9a). That is, the signs of γ_{xxxx} at the CC levels obtained using the extended basis sets, which are necessary for a sufficient description of the feature of charge distribution for the anion radical, are shown to be positive though those of γ_{xxxx} obtained using the standard basis sets are shown to be negative.

Figure 9b shows that the sign of γ_{xxxx} for $CH(CH_2)_2$ is positive and the electron-correlation effect on the γ_{xxxx} beyond the MP2 level is relatively small. Both the positive sign and relatively small electron-correlation dependence of γ_{xxxx} for $CH(CH_2)_2$ coincide with our prediction using SRIP, which hardly has contribution to the stability of the ground state due to the charge separation of the resonant structures for $CH(CH_2)_2$ (see Figure 3b).

The signs of γ_{xxxx} for $NH(CH_2)_2^+$ at the MPn ($n = 2-4$) levels are shown to be negative similarly to the case of $BH(CH_2)_2^-$ (see Figure 9c). On the other hand, the γ_{xxxx} of $NH(CH_2)_2^+$ remains negative at the CC levels. This indicates that the |type (II)| contribution in $NH(CH_2)_2^+$ exceeds the |type (III)| contribution at the CC levels. These features also coincides with our prediction based on the large SRIP contribution for $NH(CH_2)_2^+$.

5.3. γ Density Analysis. Figures 10−12 show the results of γ_{xxxx} density analysis for the three-center radicals obtained by the HF, MP2, QCISD, and B3LYP methods using 6-311G+f/d basis set. A plane at which the γ_{xxxx} densities are drawn is located at 1.0 au above the molecular plane since we focus on the contribution of π-electrons to the γ_{xxxx}.

As shown in Figure 10a−d, the γ_{xxxx} density distributions of $BH(CH_2)_2^-$ at the HF, MP2, QCISD, and B3LYP levels have a similar distribution pattern, in which the inner and the outer regions provide the negative and the positive contributions to the γ_{xxxx}, respectively. Since the contribution of the outer region is found to be larger than that of the inner region, the γ_{xxxx} at the HF, QCISD, and B3LYP levels become positive in sign. In contrast, at the MP2 level, the inner contribution (negative) is found to exceed the outer contribution (positive), so that the γ_{xxxx} at the MP2 level becomes negative. The feature that the contribution at the MP2 level is different from other results is similar to that for the anionic one-center radical (BH_3^-). As shown in Figure 10a,c, although the γ_{xxxx} density distribution pattern at the QCISD level is shown to be similar to those at the HF level, the outer γ_{xxxx} density region at the QCISD level is shown to expand. The change in the shape of γ_{xxxx} density distribution causes the difference between the magnitude of γ_{xxxx} at the HF level and that at the QCISD level. Although the outer region of γ_{xxxx} density distribution for $BH(CH_2)_2^-$ at the B3LYP level is shown to be slightly enhanced compared to that at the QCISD level, the total γ_{xxxx} value and its density distribution feature well coincide with those at the QCISD level.

Figure 11 shows the γ_{xxxx} density distribution of $CH(CH_2)_2$. Similarly to the neutral one-center radical case (CH_3), there is no noticeable difference in the γ_{xxxx} density distributions of $CH(CH_2)_2$ among at the HF, MP2, and QCISD levels (see Figure 11a,c). This indicates that the electron-correlation effect on the γ_{xxxx} density distribution of $CH(CH_2)_2$ is relatively small. This result is considered to be in good agreement with the prediction using SRIP contribution to the ground state of $CH(CH_2)_2$. It is noted that the γ_{xxxx} density distribution of $CH(CH_2)_2$ at the B3LYP level (Figure 11d) more resembles that at the QCISD level in the magnitude of γ_{xxxx} densities compared with the HF and MP2 cases. Considering the results for the neutral one- and three-center radicals, the B3LYP method is suggested to be able to reproduce the qualitative features of γ density distributions of neutral radical systems.

From the remarkable changes in the γ_{xxxx} distributions for $NH(CH_2)_2^+$ at the HF and MP2 levels (Figure 12, a and b), the electron-correlation effects on the γ_{xxxx} density distributions of $NH(CH_2)_2^+$ are found to be enormously large. Although there are only two γ_{xxxx} density distribution regions at the HF level (Figure 12a), the regions of which provide positive contribution to the γ_{xxxx} of $NH(CH_2)_2^+$, six γ_{xxxx} density distribution regions involving the negative contribution regions appear at the MP2 and QCISD levels (Figure 12b,c). Since the negative contributions in the outer regions at the MP2 and QCISD levels are

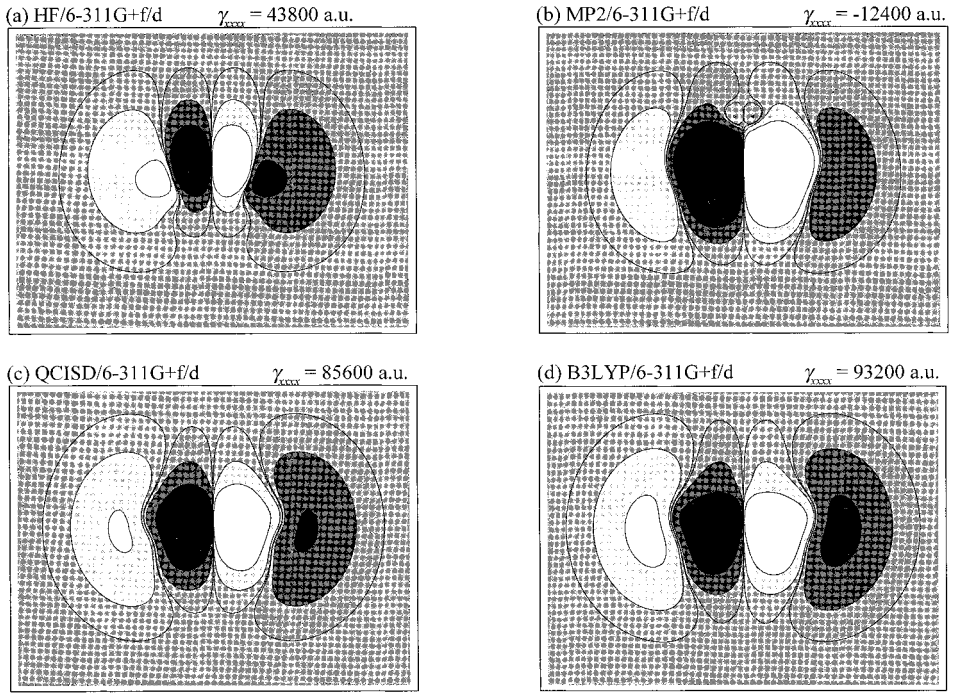

Figure 10. Contour plots of $\rho^{(3)}_{xxx}(\boldsymbol{r})$ distribution on the plane located at 1.0 au above the molecular plane for $BH(CH_2)_2^-$. Contours are drawn at 50.0, 10.0, 1.0, −1.0, −10.0, and −50.0 au. Lighter areas represent the spatial regions with larger $\rho^{(3)}_{xxx}(\boldsymbol{r})$ values.

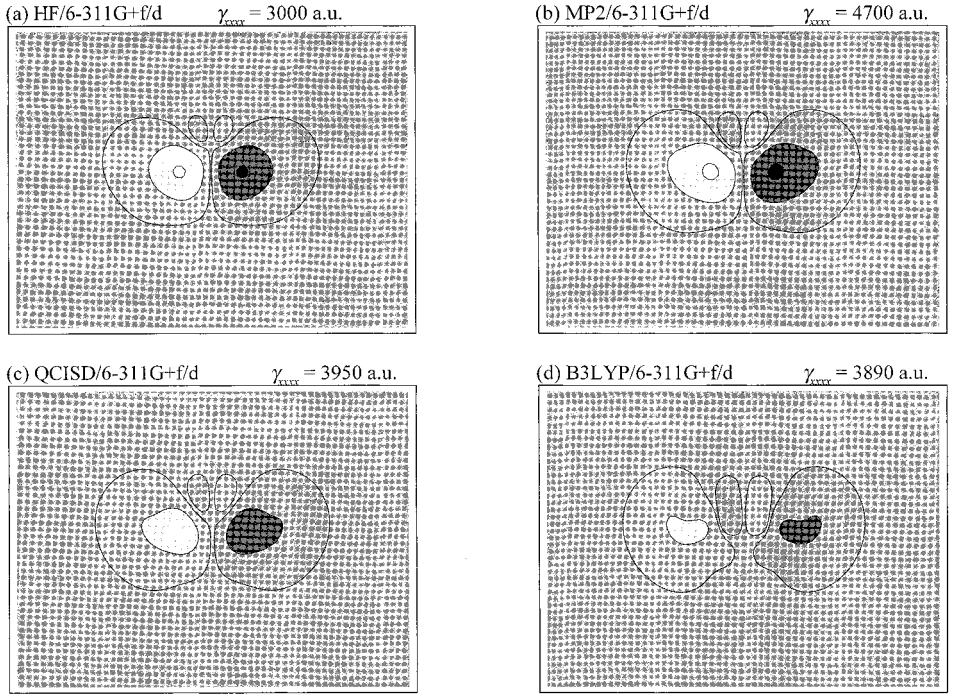

Figure 11. Contour plots of $\rho^{(3)}_{xxx}(\boldsymbol{r})$ distribution on the plane located at 1.0 au above the molecular plane for $CH(CH_2)_2$. Contours are drawn at 50.0, 10.0, 1.0, −1.0, −10.0, and −50.0 au. Lighter areas represent the spatial regions with larger $\rho^{(3)}_{xxx}(\boldsymbol{r})$ values.

shown to slightly exceed the positive contributions in the inner regions, relatively small positive γ_{xxxx} values are observed at the MP2 and QCISD levels. The each magnitude of positive and negative γ_{xxxx} density distribution of $NH(CH_2)_2^+$ at the MP2 level is considerably enhanced compared with that at the QCISD level though their γ_{xxxx} density distribution patterns and shapes are similar to each other. This feature is considered to lead to the fact that the magnitude of γ_{xxxx} at the MP2 level is much larger than that at the QCISD level. These remarkable changes in the magnitude and pattern of γ_{xxxx} distribution of $NH(CH_2)_2^+$ for these electron-correlation methods are considered to reflect the large SRIP contribution for this system (see Figure 3c). It is also noted that the γ_{xxxx} values and their density distributions using QCISD and B3LYP methods well coincide with each other in the signs, magnitude, and shapes of the distributions.

6. Concluding Remarks

It is found from the present study that the augmentation of diffuse and polarization functions is essential for reproducing the qualitatively converged γ_{xxxx} and its qualitative electron-correlation dependences for one- and three-center radicals,

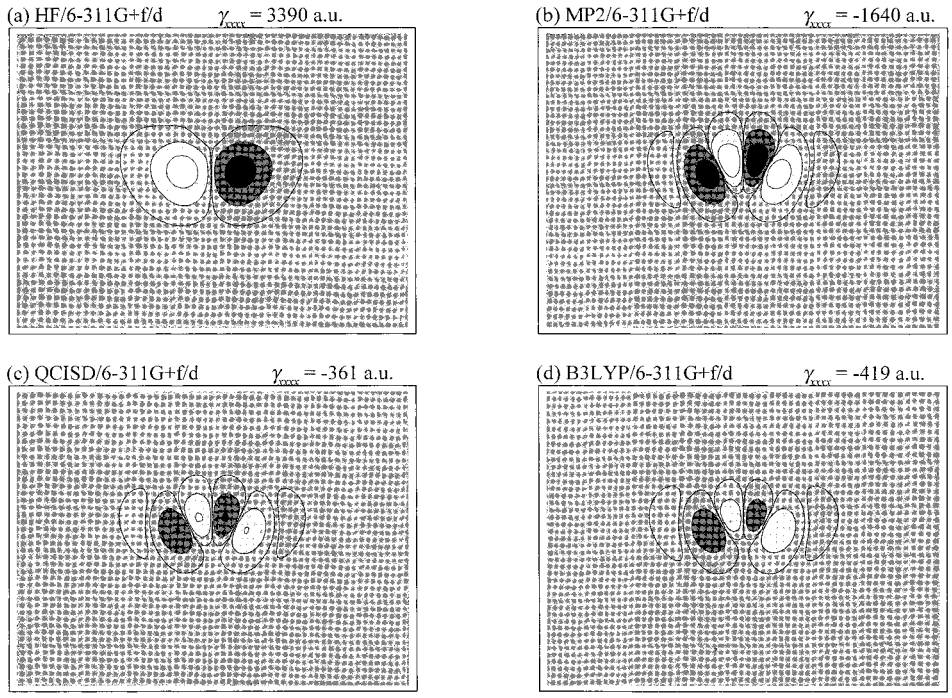

Figure 12. Contour plots of $\rho^{(3)}_{xxx}(\boldsymbol{r})$ distribution on the plane located at 1.0 au above the molecular plane for $NH(CH_2)_2^+$. Contours are drawn at 50.0, 10.0, 1.0, −1.0, −10.0, and −50.0 au. Lighter areas represent the spatial regions with larger $\rho^{(3)}_{xxx}(\boldsymbol{r})$ values.

especially for the anion radical models. It is also found that the γ_{xxxx} values of charged radicals, except for NH_3^+, exhibit remarkable electron-correlation dependences, which can be predicted based on the SRIP contributions for these charged radicals. As expected from our structure−property correlation rule using SRIP contribution, the γ_{xxxx} values for the anionic and cationic three-center radicals at the high-order electron-correlation levels, i.e., QCISD and CCSD levels, are found to be largely positive and slightly negative in sign, respectively. It is also found from the γ_{xxxx} density analysis that the differences in the magnitude of γ_{xxxx} for the one- and three-center radicals are found to reflect those in the extent of their charge distributions.

It is concluded that the γ_{xxxx} values of isoelectronic one- and three-center radicals sensitively reflect the features of the charge distributions and the degree of SRIP contributions as follows. First, the extended charge distribution region for anion radicals is considered to enhance the contribution of type (III) (positive) in eq 1. This makes the |type (III)| contribution larger than the |type (II)| contribution though the anion radicals have somewhat SRIP contribution, which enhances the type (II) contribution. This is also understood by the fact that the strong Coulomb repulsion due to the excess electron in the SRIP for the anion radical systems leads to reduced SRIP contribution, while the excess electron in the extended region causes the enhancement of the type (III) contribution involving high-lying excited states. Second, the charge polarization structures of SRIP in the neutral radicals are considered to have only slight contributions to the ground states of neutral radicals. In this case, the |type (III)| contribution is larger than the |type (II)| contribution, so that the total γ becomes positive. Third, the charged defect in three-center cation radicals is considered to enhance the SRIP contribution. In this case, the three-center cation radical ($NH(CH_2)_2^+$) exhibits negative γ_{xxxx} since the |type (II)| contribution exceeds the |type (III)| contribution. However, the magnitude of the γ_{xxxx} for $NH(CH_2)_2^+$ is shown to be small at the CC levels. This is considered to be caused by the fact that the extent of charge distribution is restricted to small regions for the cationic radicals.

From the present results, we here mention the applicability of the B3LYP method to the calculation of γ for radical systems. It is elucidated that the γ_{xxxx} density distributions for cationic, neutral, and anionic one- and three-center radicals at the B3LYP level can qualitatively well reproduce those at the QCISD level. Therefore, if the exchange and correlation functionals of a DF method were more improved or tuned to the calculation of γ, the DF method could qualitatively better reproduce the γ values and their density distributions for *n*-center radical systems at the sufficiently high-order electron-correlation level.

Although our prediction of γ is based on the degree of the contribution of SRIP, the estimation of its contribution is performed in a qualitative manner in this study. In order to obtain more quantitative prediction of γ, some efficient extraction methods of the valence-bond pictures mainly contributing to the ground state would be useful.

Judging from the results in this study, the magnitude of γ for *n*-center cation radicals is presumed to be small even if the sign of γ is negative. On the other hand, *n*-center anion radicals are presumed to tend to have positive γ. However, if the charge polarization structure of a neutral *n*-center radical sufficiently contributes to the ground state, such neutral radical has a possibility of a large negative γ. The neutral five-center radical, i.e., nitronyl nitroxide radical, which have been proposed in our previous papers,[8,9,15] is considered to correspond to this case. In this system, the highly polarizable N−O unit is presumed to make it possible for the SRIP with a remarkable charge separation to significantly contribute to the ground state.

Acknowledgment. This work was supported by Grant-in-Aid for Scientific Research on Priority Areas (No. 11166239 and 10149101) from Ministry of Education, Science, Sports and Culture, Japan, and a Grant from CASIO Science Promotion Foundation.

References and Notes

(1) Prasad, P. N.; Williams, D. J. *Introduction to Nonlinear Optical Effects in Molecules and Polymers*; Wiley: New York, 1990.

(2) Brédas, J. L.; Adant, C.; Tackx, P.; Persoons, A.; Pierce, B. M. *Chem. Rev.* **1994**, *94*, 243.

(3) Kanis, D. R.; Ratner, M. A.; Marks, T. J. *Chem. Rev.* **1994**, *94*, 195.

(4) Nakano, M.; Yamaguchi, K. *Analysis of nonlinear optical processes for molecular systems*; Trends in Chemical Physics; Research Trends: Trivandrum, India, 1997; Vol. 5, pp 87−237.

(5) Nakano, M.; Yamaguchi, K. *Chem. Phys. Lett.* **1993**, *206*, 285.

(6) Nakano, M.; Kiribayashi, S.; Yamada, S.; Shigemoto, I.; Yamaguchi, K. *Chem. Phys. Lett.* **1996**, *262*, 66.

(7) Shen, Y. R. *The Principles of Nonlinear Optics*; Academic: New York, 1984.

(8) Nakano, M.; Yamada, S.; Yamaguchi, K. *Bull. Chem. Soc. Jpn.* **1998**, *71*, 845.

(9) Yamada, S.; Nakano, M.; Yamaguchi, K. *Chem. Phys. Lett.* **1997**, *276*, 375.

(10) Awaga, K.; Maruyama, Y. *Chem. Phys. Lett.* **1989**, *158*, 556.

(11) Kamada, K.; Ohta, K.; Nakamura, J.; Yamada, S.; Nakano, M.; Yamaguchi, K. *Mol. Cryst. Liq. Cryst.* **1998**, *315*, 117.

(12) Becke, A. D. *J. Chem. Phys.* **1993**, *98*, 5648.

(13) Nakano, M.; Shigemoto, I.; Yamada, S.; Yamaguchi, K. *J. Chem. Phys.* **1995**, *103*, 4175.

(14) Nakano, M.; Okumura, M.; Yamaguchi, K.; Fueno, T. *Mol. Cryst. Liq. Cryst.* **1990**, *182A*, 1.

(15) Yamada, S.; Nakano, M.; Shigemoto, I.; Yamaguchi, K. *Chem. Phys. Lett.* **1997**, *267*, 445.

(16) Nakano, M.; Yamada, S.; Yamaguchi, K. *J. Phys. Chem.*, in press.

(17) Frisch, M. J.; Trucks, G. W.; Head-Gordon, M.; Gill, P. M. W.; Wong, M. W.; Foresman, J. B.; Johnson, B. G.; Schlegel, H. B.; Robb, M. A.; Replogle, E. S.; Gomperts, R.; Andres, J. L.; Raghavachari, K.; Binkley, J. S.; Gonzalez, C.; Martin, R. L.; Fox, D. J.; Defrees, D. J.; Baker, J.; Stewart, J. J. P.; Pople, J. A. *Gaussian 94*, Revision B.1; Gaussian, Inc.: Pittsburgh, PA, 1995.

(18) Yamada, S.; Nakano, M.; Shigemoto, I.; Yamaguchi, K. *Chem. Phys. Lett.* **1996**, *254*, 158.

(19) Feynman, R. *Phys. Rev.* **1939**, *56*, 340. Epstein, S. T. *Am. J. Phys.* **1954**, *22*, 613.

(20) Nerbrant, P. O.; Roos, B. O.; Sadlej, A. J. *Int. J. Quantum Chem.* **1979**, *15*, 135.

(21) Hurst, G. J. B.; Dupuis, M.; Clementi, E. *J. Chem. Phys.* **1998**, *89*, 385.